PHYSICAL REVIEW D **92,** 015016 (2015)

Search for doubly charged Higgs bosons through vector boson fusion at the LHC and beyond

G. Bambhaniya[*]
Theoretical Physics Division, Physical Research Laboratory, Ahmedabad 380009, India

J. Chakrabortty[†]
Department of Physics, Indian Institute of Technology, Kanpur 208016, India

J. Gluza[‡] and T. Jeliński[§]
Institute of Physics, University of Silesia, Uniwersytecka 4, 40-007 Katowice, Poland

R. Szafron[‖]
Department of Physics, University of Alberta, Edmonton, Alberta T6G 2E1, Canada
(Received 23 April 2015; published 17 July 2015)

Production and decays of doubly charged Higgs bosons at the LHC and future hadron colliders triggered by a vector boson fusion mechanism are discussed in the context of the minimal left-right symmetric model. Our analysis is based on the Higgs boson mass spectrum compatible with available constraints which include flavor changing neutral current (FCNC) effects and vacuum stability of the scalar potential. Though the parity breaking scale v_R is large ($\sim$few TeV) and scalar masses which contribute to FCNC effects are even larger, a consistent Higgs boson mass spectrum still allows us to keep doubly charged scalar masses below 1 TeV which is an interesting situation for LHC and future circular collider (FCC). We have shown that the allowed Higgs boson mass spectrum constrains the splittings ($M_{H_1^{\pm\pm}} - M_{H_1^{\pm}}$), closing the possibility of $H_1^{\pm\pm} \to W_1^{\pm} H_1^{\pm}$ decays. Assuming that doubly charged Higgs bosons decay predominantly into a pair of same-sign charged leptons through the process $pp \to H_{1/2}^{\pm\pm} H_{1/2}^{\mp\mp} jj \to \ell^{\pm}\ell^{\pm}\ell^{\mp}\ell^{\mp} jj$, we find that for the LHC operating at $\sqrt{s} = 14$ TeV with an integrated luminosity at the level of 3000 fb^{-1} (HL-LHC), there is practically no chance to detect such particles at the reasonable significance level through this channel. However, at 33 TeV HE-LHC and (or) 100 TeV FCC-hh, a wide region opens up for exploring the doubly charged Higgs boson mass spectrum. In FCC-hh, the doubly charged Higgs bosons mass up to 1 TeV can be easily probed.

DOI: 10.1103/PhysRevD.92.015016 PACS numbers: 12.60.-i, 12.60.Fr, 14.80.Fd, 14.80.Ec

I. INTRODUCTION

Weak vector boson fusion (VBF) processes were suggested quite some time ago in the context of Higgs searches [1–3]. They are characterized by the presence of two jets with large transverse momentum (p_T) in the forward region in opposite hemispheres along with other observables, like charged leptons. In fact, many interesting standard model (SM) processes, e.g. diffractive interactions, low-x QCD physics, VBF Higgs production, and photoproduction are also accompanied by production of forward particles. Interestingly, the LHC has a very rich "forward physics" program and for the necessary investigation there are dedicated detectors like LHCf [4] and (or) FP420 [5]. Due to uncertainties in jet tagging, the efficiency is relatively low and, thus, the significance of these channels is rather suppressed. Nevertheless, from the discovery perspective, many beyond standard models (BSM) can also be tested using forward jets. Such related studies are also important for dark matter searches through mono-jet plus missing energy [6–8].

In this paper we continue [9–11] a dedicated analysis of the minimal left-right symmetric model (MLRSM) [12–14], aiming at an exhaustive exploration of interesting BSM signals at present and future hadron colliders.[1] For many reasons, the parity breaking scale v_R of the right $SU(2)$ group in MLRSM must be already around $\mathcal{O}(10)$ TeV [9–11,18,19]. However, as discussed recently in [10,11], in such models charged Higgs bosons can have masses at the much lower level of a few hundred GeV, and that scenario is still consistent with experimental data. In this case, it is imperative to cover all possible scenarios, and

[*]gulab@prl.res.in
[†]joydeep@iitk.ac.in
[‡]janusz.gluza@us.edu.pl
[§]tomasz.jelinski@us.edu.pl
[‖]szafron@ualberta.ca

[1]The main features of this model are equal $SU(2)$ left and right gauge couplings, $g_L = g_R$, and a scalar potential which contains a bidoublet and two triplet scalar multiplets, considered for the first time in [15]; see also [16,17].

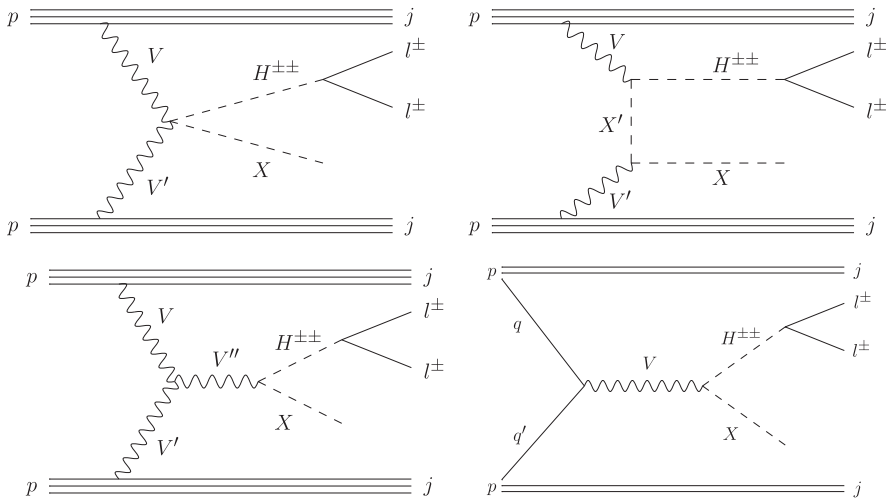

FIG. 1. Basic processes which lead to $H^{\pm\pm}$ pair production. In the first three diagrams, $H^{\pm\pm}$ is produced through fusion of two vector bosons V and V'. Each of them can be $W^{\pm}$, Z^0 or γ. The second product of the fusion, scalar X, is $H^{\pm\pm}$, $H^{\pm}$ or H^0, depending on the configuration of colliding vector bosons. Analogously, scalar X' and vector boson V'' can be identified once V and V' are specified. In the last diagram, $H^{\pm\pm}$ is produced through collision of two quarks q and q' in the Drell-Yan process. The second product of the decay, scalar X, can be identified as $H^{\pm\pm}$, $H^{\pm}$ or H^0 once V is specified.

their potential effects at the LHC should be analyzed carefully. Interestingly enough, a recent CMS study [20] can be interpreted as favoring right-handed currents.

In our previous analyses we have worked with the scalar mass spectra which are compatible with the unitarity of the potential parameters, the large parity breaking scale v_R and the severe bounds on neutral scalar masses $(M_{H_1^0}, M_{A_1^0})$ derived from flavor changing neutral currents (FCNCs). In this work we have further implemented another necessary condition: vacuum stability of the scalar potential. It appears that even after taking into account all these constraints, the consistent scalar mass spectra can accommodate doubly charged Higgs boson masses in a region which can be explored by the LHC.

In the past, we have focused on searches for multilepton signals associated with any number of jets; i.e., there was no jet veto. Here, the analysis of possible VBF-type signals with four leptons and two jets using suitable VBF cuts is presented.

We have used our version of the left-right symmetric model implemented in FeynRules (v2.0.31) [21,22]. The general signal and background analyses for multilepton and tagged forward jets are performed using ALPGEN (v2.14) [23], Madgraph (v2.2.2) [24] and PYTHIA (v6.421) [25].

II. POSSIBLE PROCESSES WHICH IDENTIFY DOUBLY CHARGED HIGGS THROUGH VBF IN MLRSM

There are many interesting channels in which doubly charged Higgs particles can be produced in MLRSM. In the hadron collider, productions of doubly charged Higgs particles crucially depend on their couplings with vector bosons. These charged scalars ($H^{\pm\pm}$) are produced either through neutral and charged currents or fusion processes. Representative classes of diagrams which contribute to $H^{\pm\pm}$ productions associated with two jets are given in Fig. 1.

If $X = H^{\pm\pm}$ in Fig. 1, then doubly charged Higgs particles are produced in pairs. Assuming further that $H^{\pm\pm}$ decays predominantly into leptons, a signal of four leptons associated with two forward jets in the final state is foreseen, $pp \to H^{\pm\pm}_{1/2} H^{\mp\mp}_{1/2} jj \to \ell^{\pm}\ell^{\pm}\ell^{\mp}\ell^{\mp} jj$. In the Drell-Yan case also [see the diagram in Fig. 1(d)], if $X = H^{\pm\pm}$, a four leptons plus two jets signal is possible, though its contribution is suppressed once the VBF cuts are activated.

We should also mention that vector boson fusion diagrams interfere substantially with Bremsstrahlung-like (or Drell-Yan) processes [26].

Here we focus on the pair production of doubly charged scalars associated with two forward jets. As mentioned already, this signature can be promising since LHC has dedicated search channels for tagged forward jets. VBF processes with doubly charged Higgs bosons have been considered lately in [27] with the main focus on three lepton signals with missing energy and in [28] where doubly charged Higgs bosons decay into same-sign W bosons. In [27] there is also an interesting discussion on scalar corrections to the self-energy of $W_L^{\pm}$ and the $\Delta\rho_{\rm EW}$ parameter. It has been argued that there exist severe constraints on the charged scalar mass splitting. However, in our opinion conclusions based on partial results and a single class of (scalar) diagrams can be deceptive; thus, we need to consider complete calculations

including renormalization. We recall a series of papers on the one-loop corrections to the muon decay in MLRSM, starting with qualitative results [29,30] and finishing with quantitative analysis [31]. The upshot of all these analyses, important for our present discussion, is that there is a strong fine-tuning between contributions to $\Delta\rho_{\rm EW}$ from different classes of nonstandard particles: Higgs and additional gauge *bosons* and heavy neutrinos (*fermions*). By their nature, cancellations among bosonic and fermionic types of diagrams are present, and a change of mass spectrum of the Higgs bosons can be compensated for by different choices of v_R scale (gauge bosons) and masses of heavy neutrinos. These analyses in the context of the LHC have been considered in detail in [9].

III. CONSTRAINTS ON α_3 AND $\delta\rho$: ADDING VACUUM STABILITY CONDITION

Analysis of the LHC data provides lower limits on the doubly charged Higgs mass [32] depending on the leptonic decay branching fractions. In the scenario where $\mathrm{BR}(H^{++}\to e^+e^+)=\mathrm{BR}(H^{++}\to\mu^+\mu^+)\approx 0.5$, that limit is $M_{\rm LHC}=M_{H^{\pm\pm}}\approx 450$ GeV; see Fig. 2 for details.

Limits on the MLRSM potential parameters have been discussed lately in [11]. Similar to the earlier case, we focus on the α_3 and $\delta\rho=\rho_3-2\rho_1$ parameters, which are important for the scalar mass spectrum (all notations are as in [10,11]). First, to suppress FCNC effects generated by H_1^0 and A_1^0, we assume[2] that their mass is bigger than $M_{\rm FCNC}=10$ TeV. Because $M^2_{H_1^0,A_1^0}=\alpha_3 v_R^2/2$, this results in the following lower limit on α_3:

$$\alpha_3\geq\frac{2M^2_{\rm FCNC}}{v_R^2}. \tag{1}$$

Taking into account that $M^2_{H_1^{\pm\pm}}=(\delta\rho v_R^2+\alpha_3\kappa^2)/2$, one gets

$$\alpha_3\geq\frac{1}{\kappa^2}(2M^2_{\rm LHC}-\delta\rho\, v_R^2), \tag{2}$$

where $\kappa=246$ GeV is the electroweak symmetry breaking scale. The third constraint originates from the necessary condition of the boundedness of the potential [39]:

$$\alpha_3\leq\sqrt{8\lambda_1(4\pi-\delta\rho)}. \tag{3}$$

The value of λ_1 is fixed by the lightest neutral Higgs boson mass as $M^2_{H_0^0}=2\lambda_1\kappa^2$.

[2]To our knowledge, their effects have been discussed for the first time in the context of left-right models in [33]; see also [9,18,34–36] and recently [37]. In general, their masses need to be at least of the order of 10 TeV, though some alternatives also have been considered in [38].

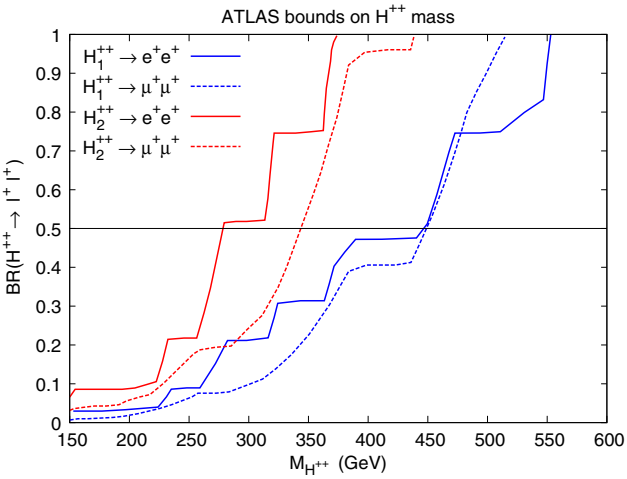

FIG. 2 (color online). Exclusion limits on the masses of doubly charged scalars from the ATLAS analysis, depending on their leptonic branching ratios. The lepton flavor violating modes are not shown here, as they are not concerned with the purpose of our analysis. This plot is based on Fig. 5 in [32].

Now it is interesting and important to ask what is the maximum allowed mass splitting $\Delta M=M_{H_1^{\pm\pm}}-M_{H_1^{\pm}}$ that will be consistent with the bounds on $(\alpha_3,\delta\rho)$ derived above. Such queries cannot be unnoticed from a phenomenological perspective because only for $\Delta M>M_{W_1}$ can the doubly charged Higgs have the following decay: $H_1^{\pm\pm}\to H_1^{\pm}W_1^{\pm}$. This has a massive impact on the decay branching ratios of $H^{\pm\pm}$. It is straightforward to check that the biggest ΔM is reached for $\delta\rho$, saturating both inequalities in Eqs. (2) and (3) which imply

$$\frac{1}{\kappa^2}(2M^2_{\rm LHC}-\delta\rho v_R^2)=\sqrt{8\lambda_1(4\pi-\delta\rho)}. \tag{4}$$

The physical solution to this equation and the corresponding maximal value of ΔM is

$$\delta\rho=\frac{2(M^2_{\rm LHC}-\sqrt{8\pi\lambda_1}\kappa^2)}{v_R^2}(1+\cdots),$$
$$\Delta M=\Delta M_\infty(1+\cdots), \tag{5}$$

where '…' stands for corrections of the order of $\mathcal{O}(M^2_{\rm LHC}/v_R^2,\kappa^2/v_R^2)$. One can check that ΔM depends on v_R very weakly and is nearly equal to the asymptotic value $\Delta M_\infty=\lim_{v_R\to\infty}\Delta M=M_{\rm LHC}-\sqrt{M^2_{\rm LHC}-\sqrt{2\pi\lambda_1}\kappa^2}\approx 65.3\,\mathrm{GeV}$, for $M_{\rm LHC}=450$ GeV. As $\partial_{v_R}\Delta M>0$, this implies that on-shell decay $H_1^{\pm\pm}\to H_1^{\pm}W_1^{\pm}$ is kinematically forbidden regardless of the scale v_R. Interestingly, we came to the same conclusion as in [27], but based on different kinds of arguments. There is another consequence of the requirement that the scalar potential is bounded from below. Namely, one can show that, using Eqs. (1) and (3), in the

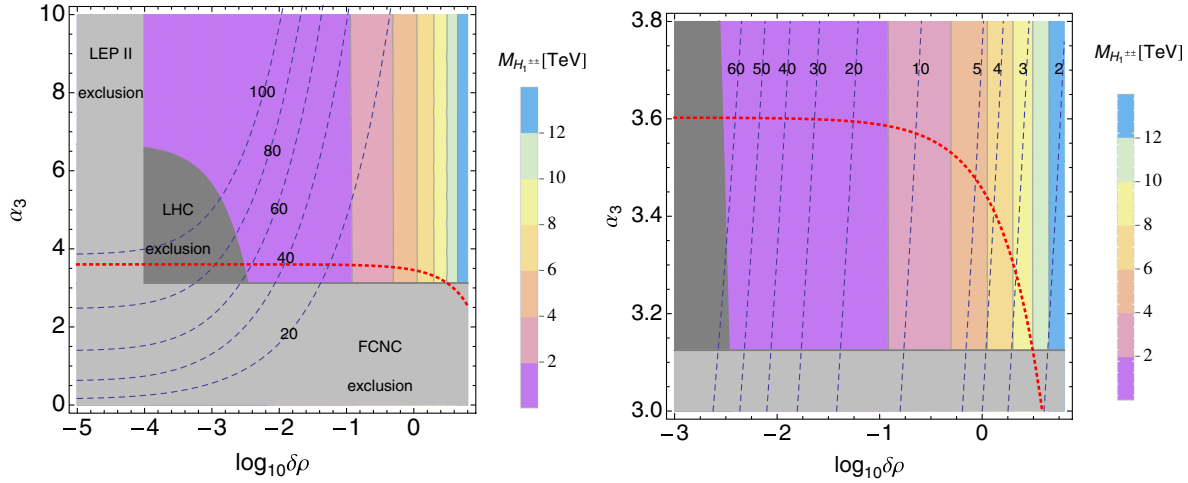

FIG. 3 (color online). (left panel) Dependence of the $H_1^{\pm\pm}$ mass (in TeV) on $\delta\rho$ and α_3 for $v_R = 8$ TeV. The parameter space $(\delta\rho, \alpha_3)$ is divided into colored regions where mass of $H_1^{\pm\pm}$ is characterized according to the attached legend. Shaded regions are excluded due to FCNC, LHC and LEP constraints; see Eqs. (1) and (2) and Refs. [11,40], respectively. The parameter space above the red-dotted line is disfavored due to the unboundedness of the scalar potential; see Eq. (3). Blue, dashed lines represent sets of points $(\delta\rho, \alpha_3)$ for which mass splitting $(M_{H_1^{\pm\pm}} - M_{H_1^{\pm}})$ is 100, 80, 60, 40 and 20 GeV respectively. (right panel) Detailed view of the allowed part of parameter space with refined mass splitting lines.

allowed parameter space there is an upper limit on the $H_1^{\pm\pm}$ mass:

$$M_{H_1^{\pm\pm}} \leq \frac{1}{2}\sqrt{8\pi v_R^2 - \frac{M_{\rm FCNC}^4}{\lambda_1 v_R^2}(1+\cdots)} \approx 9.98 \text{ TeV}, \quad (6)$$

where "…" stands for the corrections of order of $\mathcal{O}(\kappa^2/v_R^2)$. The maximal value of $M_{H_1^{\pm\pm}}$ is reached for $\delta\rho$ satisfying $\sqrt{8\lambda_1(4\pi - \delta\rho)} = 2M_{\rm FCNC}^2/v_R^2$ and $\alpha_3 = 2M_{\rm FCNC}^2/v_R^2$, which correspond to the intersection point of lines restricting regions defined by Eqs. (1) and (3). The situation is summarized in Fig. 3. Naturally, the minimal value of the $H_1^{\pm\pm}$ mass in the discussed setup is $M_{\rm LHC}$. For the sake of completeness, let us note that if there are no experimental limits on $M_{H_1^{\pm\pm}}$ and H_3^0, then the lowest possible mass of $H_1^{\pm\pm}$ consistent with the vacuum stability bound, Eq. (3), would be $\sqrt{2\sqrt{\pi}M_{H_0^0}v} \approx 330$ GeV, which corresponds to $\delta\rho \to 0$ and $\alpha_3 \to \sqrt{32\pi\lambda_1}$. On the other hand, the MLRSM does not provide any relevant constraints on the $H_2^{\pm\pm}$ mass.[3] We would like to mention that when ρ_2 satisfies

$$\rho_2 < \frac{1}{4}\min(\alpha_3, \delta\rho) + \frac{1}{2}\frac{M_{W_{1,2}}^2}{v_R^2} - \frac{1}{8}\alpha_3\frac{\kappa^2}{v_R^2}, \quad (7)$$

then a similar type of decay of $H_2^{\pm\pm}$ is kinematically forbidden as $H_2^{\pm\pm}$ is too light to decay into $H_2^{\pm}$ and $W_{1,2}^{\pm}$, respectively; see the benchmarks in the next section.

[3]The only constraint which could arise is $M_{H_2^{\pm\pm}} < 2\sqrt{6\pi}v_R \approx 40$ TeV for $v_R = 8$ TeV. It comes from the assumption that scalar potential parameter ρ_2 is in the perturbative regime $\rho_2 < 4\pi$.

IV. PREDICTIONS FOR $pp \to H_{1/2}^{\pm\pm}H_{1/2}^{\mp\mp}jj \to \ell^{\pm}\ell^{\pm}\ell^{\mp}\ell^{\mp}jj$ IN MLRSM

Before we discuss our simulated results, selection criteria should be defined, which are crucial for extracting proper signals and reducing the SM background. For selecting leptons, we use the same criteria as defined in previous papers [10,41], which are read as follows:

(i) Lepton identification criteria: pseudorapidity $|\eta_\ell| < 2.5$ and $p_{T\ell} > 10$ GeV.
(ii) Detector efficiency for charged leptons:
electron (either $e^{\pm}$): 0.7 (70%).
muon (either $\mu^{\pm}$): 0.9 (90%).
(iii) Smearing of muon p_T and electron energy are implemented in PYTHIA.
(iv) Lepton-lepton separation: $\Delta R_{ll} \geq 0.2$.
(v) Lepton-photon separation: $\Delta R_{l\gamma} \geq 0.2$ where all the photons have $p_{T\gamma} > 10$ GeV.
(vi) We have implemented a Z veto to suppress the SM background, and this has a larger impact while reducing the background for the four-lepton without missing energy. This veto reads as follows: The same flavored but opposite sign lepton pair invariant mass $m_{\ell_1\ell_2}$ must be sufficiently away from the SM Z-boson mass, say, $|m_{\ell_1\ell_2} - M_{Z_1}| \geq 6\Gamma_{Z_1} \sim 15$ GeV.
(vii) Lepton-jet separation: The separation of a lepton with all nearby jets must satisfy $\Delta R_{lj} \geq 0.4$. If this is not satisfied, then that lepton is not counted as a lepton. For completeness, we must mention that jets are constructed from hadrons using PYCELL within PYTHIA.
(viii) Hadronic activity cut: this cut is applied to consider only those leptons that have much less hadronic activity around them. Each lepton should have

TABLE I. Selection criteria for the forward jets. The two highest p_T jets p_{Tj_1}, p_{Tj_2} are chosen as the VBF forward jets.

Cuts	p_{Tj_1}, p_{Tj_2}	$\lvert\eta_{j_1} - \eta_{j_2}\rvert$	$m_{j_1 j_2}$	$\eta_{j_1} * \eta_{j_2}$
VBF	≥ 50	> 4	500	< 0

hadronic activity which is accounted as $\frac{\sum p_{T_{\text{hadron}}}}{p_{T_l}} \leq 0.2$ within the cone of radius 0.2 around the lepton;

(ix) Hard p_T cuts for four lepton events: $p_{Tl_1} > 30$ GeV, $p_{Tl_2} > 30$ GeV, $p_{Tl_3} > 20$ GeV, $p_{Tl_4} > 20$ GeV.

The parton distribution function (PDF) for protons is defined by CTEQ6L1 [42]. After satisfying the above selection criteria, additional cuts are applied to identify the forward jets. The detail of these VBF cuts are depicted in Table I.

Considering the constraints on potential parameters discussed in Sec. III, in Fig. 4 the results are presented for the doubly charged Higgs production process with two jets as a function of their mass. While computing the MLRSM mass spectrum, we have set $v_R = 8$ TeV (which leads to $M_{W_2} = 3.76$ TeV). The analyses are performed for the LHC with 14 TeV collision energy considering the high luminosity HL-LHC option [43] as well as for future scenarios such as HE-LHC with center of mass energy 33 TeV [43,44] or the 100 TeV FCC-hh facility [45–48]. The cross section for this process has been computed with a large p_{T_j} and VBF cuts as defined in Table I.

As an example of a representative Higgs mass spectrum (benchmark) used in calculations, we assume degenerate doubly charged Higgs masses $M_{H_1^{\pm\pm}} = M_{H_2^{\pm\pm}} = 500[1000]$ GeV where masses of remaining scalar particles compatible with results of Sec. III can be chosen as (in GeV):

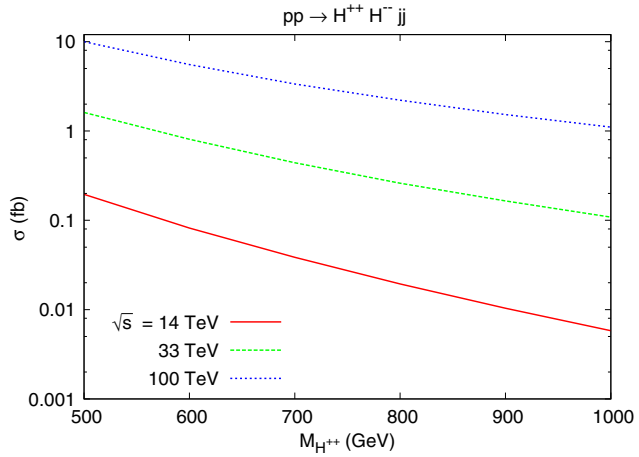

FIG. 4 (color online). Dependence of cross sections (σ) with the masses of doubly charged scalars for the process $pp \to H^{++}H^{--}jj$ for different center of mass energies: 14 TeV (red-solid), 33 TeV (green-dashed), and 100 TeV (blue-dotted), respectively.

$$M_{H_0^0} = 125[125], \qquad M_{H_1^0} = 10431[10431], \tag{8}$$

$$M_{H_2^0} = 27011[27011], \qquad M_{H_3^0} = 384[947], \tag{9}$$

$$M_{A_1^0} = 10437[10437], \qquad M_{A_2^0} = 384[947], \tag{10}$$

$$M_{H_1^\pm} = 446[974], \qquad M_{H_2^\pm} = 10433[10433]. \tag{11}$$

This spectrum is obtained with the following set of potential parameters ($v_R = 8$ TeV):

$$\lambda_1 = 0.129[0.129], \qquad \lambda_2 = 0[0], \tag{12}$$

$$\lambda_3 = 1[1]\lambda_4 = 0[0], \tag{13}$$

$$\alpha_1 = 0[0], \quad \alpha_2 = 0[0], \quad \alpha_3 = 3.4[3.4], \tag{14}$$

$$\rho_1 = 5.7[5.7], \qquad \rho_2 = 0.00115[0.00701], \tag{15}$$

$$\rho_3 = 11.405[11.428]. \tag{16}$$

The cross sections for the following process at the parton level with minimal imposed cuts are given as follows:

$$\sigma(pp \to H_{1/2}^{\pm\pm} H_{1/2}^{\mp\mp} jj \to \ell^\pm \ell^\pm \ell^\mp \ell^\mp jj) = \begin{cases} 4.04[0.12] \times 10^{-2} \text{ fb} & \text{for } \sqrt{s} = 14 \text{ TeV}, \\ 45.30[3.36] \times 10^{-2} \text{ fb} & \text{for } \sqrt{s} = 33 \text{ TeV}, \\ 282.80[31.76] \times 10^{-2} \text{fb} & \text{for } \sqrt{s} = 100 \text{ TeV}, \end{cases} \tag{17}$$

where $\ell = e, \mu$. These minimal cuts are e.g. minimum p_T cuts for leptons and jets such that they are identified as observable in the detector and do not contribute to missing energy.

The result in Eq. (17) is further processed using the VBF cuts defined in Table I, and the final cross sections are:

$$\sigma(pp \to H_{1/2}^{\pm\pm} H_{1/2}^{\mp\mp} jj \to \ell^\pm \ell^\pm \ell^\mp \ell^\mp jj) = \begin{cases} 0.54[0.01] \times 10^{-2} \text{ fb} & \text{for } \sqrt{s} = 14 \text{ TeV}, \\ 6.21[0.40] \times 10^{-2} \text{ fb} & \text{for } \sqrt{s} = 33 \text{ TeV}, \\ 37.01[3.54] \times 10^{-2} \text{ fb} & \text{for } \sqrt{s} = 100 \text{ TeV}. \end{cases} \tag{18}$$

For the sake of completeness, let us display contributions from two intermediate channels[4] with the default cuts in MADGRAPH (MG):

[4]In [10] we wrongly assigned $H_1^{\pm\pm}$ with right triplet and $H_2^{\pm\pm}$ with left triplet in Eq. (A.13). We would like to thank Juan Carlos Vasquez for directing our attention to this fact as he considered this process in [49].

$$\sigma(pp \to H_1^{\pm\pm} H_1^{\mp\mp} jj) = \begin{cases} 11.16[0.39] \times 10^{-2}\ \text{fb} & \text{for } \sqrt{s} = 14\ \text{TeV}, \\ 90.87[7.05] \times 10^{-2}\ \text{fb} & \text{for } \sqrt{s} = 33\ \text{TeV}, \\ 599.70[73.28] \times 10^{-2}\ \text{fb} & \text{for } \sqrt{s} = 100\ \text{TeV}, \end{cases} \quad (19)$$

and

$$\sigma(pp \to H_2^{\pm\pm} H_2^{\mp\mp} jj) = \begin{cases} 8.35[0.19] \times 10^{-2}\ \text{fb} & \text{for } \sqrt{s} = 14\ \text{TeV}, \\ 71.20[3.81] \times 10^{-2}\ \text{fb} & \text{for } \sqrt{s} = 33\ \text{TeV}, \\ 401.40[37.43] \times 10^{-2}\ \text{fb} & \text{for } \sqrt{s} = 100\ \text{TeV}. \end{cases} \quad (20)$$

As one can see, the cross sections in Eqs. (19) and (20) are larger than these given in Eq. (17). The reason for this is while computing the cross section for the leptonic final state, i.e., Eq. (18), all the selection cuts are incorporated and that reduces the cross section by a large amount.

Some technical details related to the computing method are in order here. At the MG level, one can control the gluon contributions using option QCD = 0. The cross section for $pp \to H_{1,2}^{\pm\pm} H_{1,2}^{\mp\mp} jj$ with switched off gluons turns out to be about 5 times smaller than for that with gluons. Hence, QCD contributions to that signal are really important. However, in both cases, distributions of the rapidity (y) of jets are quite different. Allowing for gluons, they are peaked around $y = 0$, which implies that jets are emitted mostly perpendicular to the beam. Otherwise, rapidities are peaked around $|y| \sim 3$ and $|y_1 - y_2| \sim 5$; i.e., there are two back-to-back jets emitted along the beam. Hence, setting QCD = 0 allows us to preselect processes which are consistent with VBF cuts. Effectively, it shortens computing time.[5]

Let us comment on the $H^{\pm\pm}$ decay scenario used in the calculations. It is assumed that the decay of $H^{\pm\pm}$ is dominantly into a pair of the same-sign and same-flavor charged leptons (for all possibilities within MLRSM, see [10]). In other words, it is assumed that the Yukawa coupling matrix of doubly charged scalar $H_2^{\pm\pm}$ with charged leptons is diagonal. Assuming no mixed leptonic decay modes ($e\mu$), i.e., no lepton flavor violation, the coupling of doubly charged scalar $H_2^{\pm\pm}$ with charged leptons in MLRSM is proportional to the heavy neutrino mass of the corresponding lepton generation. Thus the $ee, \mu\mu$ decay modes will be larger compared to the $\tau\tau$ case if the first and second generations of right-handed neutrinos are more massive than the third-generation one. This point has been clarified and shown numerically in Fig. 2.5 in Ref. [10]. In the present analysis, the masses of the first two generations of right-handed neutrinos are taken to be 3 TeV and the mass of the third one is at the level of 800 GeV. As $v_R = 8$ TeV, the Yukawa couplings are within the perturbative limit. If the $\tau\tau$ decay mode would be larger, predictions given here should be rescaled properly using corresponding branching ratios (for instance, in the democratic three-generation case, the branching ratio for the ee and $\mu\mu$ channels would be decreased by about 15% each).

The SM background at the LHC for the signal $4\ell + 2$ jets is accounted from the process $pp \to ZZ(\gamma\gamma, Z\gamma)jj \to \ell^+\ell^-\ell^+\ell^- jj$. We have noted that after implementation of the selection cuts, the dominant background is contributed from the $pp \to ZZjj \to \ell^+\ell^-\ell^+\ell^- jj$ process.

For $\sqrt{s} = 14$, 33, 100 TeV pp collisions, the SM background is given in Table II both at the parton level and after hadronization and passing through implemented cuts.

We can see that the background is suppressed very effectively. The results in Table II are obtained in the leading order; electroweak corrections can change the results not more than 10% [50] which can change the significance of signals at the level of about one percent at most.

Finally, to judge the strength of the MLRSM signals we decided to show the dependence of the significance of the result as a function of the integrated luminosity. As can be seen in Fig. 5 (left-top), a comfortable value of the significance at the level of 5 can be reached for $M_{H^{\pm\pm}} = 500$ GeV in pp collisions with

(i) $\sqrt{s} = 100$ TeV and with 100 fb^{-1} integrated luminosity;
(ii) $\sqrt{s} = 33$ TeV and with 700 fb^{-1} integrated luminosity.

No signal at this significance level (∼5) can be reached with $\sqrt{s} = 14$ TeV pp collisions, even if the integrated luminosity is around 3000 fb^{-1}.

In Fig. 5 (right-top) we can see that doubly charged Higgs bosons with masses up to $M_{H^{\pm\pm}} = 700$ GeV with significance at the level of 5 can be probed for both center of mass energy 33 and 100 TeV with integrated luminosities around 3000 and 300 fb^{-1}, respectively. In Fig. 5 (left-bottom) it is evident that the 1 TeV doubly charged scalar can be probed with a significance of 5 only

TABLE II. Standard model cross section in fb for $\ell^+\ell^-\ell^+\ell^- jj$ final state and $\sqrt{s} = 14$, 33, 100 TeV LHC. The cuts are suitably applied, see Sec. IV, to compute the SM background at the parton level and after incorporating showering and hadronization in PYTHIA.

Process: $ZZjj$ with $\sqrt{s}$ in TeV	Cross section [fb] at parton level in MADGRAPH	Cross section [fb] after showering, and hadronization in PYTHIA
14	0.115	0.003
33	1.109	0.008
100	4.794	0.038

[5]Typical run times for generating 5×10^4 events of $pp \to H_{1/2}^{\pm\pm} H_{1/2}^{\mp\mp} jj$ and $pp \to H_{1/2}^{\pm\pm} H_{1/2}^{\mp\mp} jj \to \ell^\pm\ell^\pm\ell^\mp\ell^\mp jj$ with QCD = 0 are, respectively, about 3h and 54h on 8 core 3.4 GHz CPU.

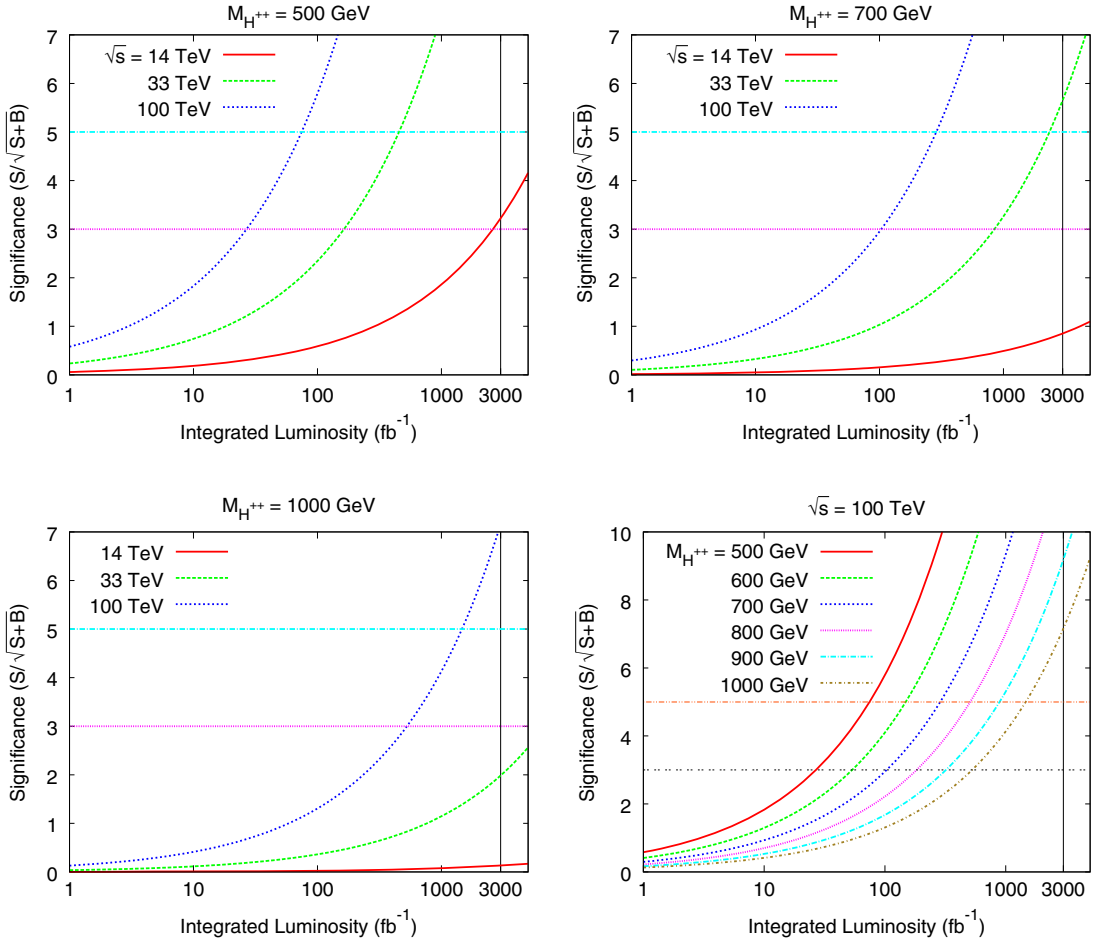

FIG. 5 (color online). Variations of significance of the signal with integrated luminosities for different energies of pp colliders and various doubly charged Higgs boson masses.

with the 100 TeV collider with luminosity at least 1000 fb^{-1}. The Fig. 5 (right-bottom) summarizes the situation for the FCC-hh collider option for three different sets of masses of doubly charged scalars: 500, 600, 700, 800, 900 and 1000 GeV. This figure also shows that significance at the level of 7 can be reached for $M_{H^{\pm\pm}} =$ 1 TeV and $\sqrt{s} = 100$ TeV with integrated luminosities around 3000 fb^{-1}. We can see that this collider opens up a very wide range of Higgs boson masses which can be explored.

V. CONCLUSIONS AND OUTLOOK

In this paper we have considered production and decays of a pair of doubly charged Higgs bosons through vector boson fusion within the MLRSM framework. To do so we have evaluated suitable benchmark points for masses of Higgs bosons, which are in agreement with several constraints coming from FCNC, vacuum stability, LEPII and recent ATLAS searches on doubly charged scalars. There are strong relations among masses of doubly and singly charged and neutral scalars which prevent us from choosing their individual values freely, leaving us with the suitable benchmarks we are using in this paper. We have further noted and shown that the splitting between the doubly ($H_1^{\pm\pm}$) and singly ($H_1^{\pm}$) charged scalars is less than M_{W_1}, irrespective of the $SU(2)_R$ breaking scale. Thus, the on-shell decay $H_1^{\pm\pm} \to H_1^{\pm} W_1^{\pm}$ is protected and the decay branching ratio of the doubly charged scalar $H_1^{\pm\pm}$ is affected.

After settling these issues regarding the spectrum, we have computed the signal cross section for the process $pp \to H_{1/2}^{\pm\pm} H_{1/2}^{\mp\mp} jj \to \ell^{\pm}\ell^{\pm}\ell^{\mp}\ell^{\mp} jj$ using realistic cuts. The necessary SM background for this final state is also evaluated. It has been shown that LHC2 even with high integrated luminosity will be not be sensitive to the VBF-like signals $H_{1/2}^{\pm\pm} H_{1/2}^{\mp\mp} jj$, even with relatively light doubly charged Higgs bosons (say, ~500 GeV). We have shown that much better perspective exists for the future FCC colliders with center of mass energies 33 and (or) 100 TeV.

In passing we would like to mention that we have used the VBF cuts as adopted in [27]. We have compared the ATLAS

and CMS (tight and loose) suggested cuts which are not very widely different from significance point of view.

Let us conclude with a comparative comment: MLRSM VBF-like signals connected with $H_2^{\pm\pm}$ scalar production (which is part of the right-handed triplet) is comparable with the $H_1^{\pm\pm}$ scalar production; see Eqs. (19) and (20). Thus the cross section for signal events are larger compare to that for type II seesaw scenario with same masses for triplet scalars. It may give a chance to disentangle between MLRSM and SM with an additional triplet, e.g. the Higgs triplet model [19,51–55], though detailed analyses are needed for comparison.

ACKNOWLEDGMENTS

The authors would like to thank Benjamin Fuks for sharing with them a modified version of FeynRules. This work is supported by the Department of Science and Technology, Government of India, under Grant Agreement No. IFA12-PH-34 (INSPIRE Faculty Award) and the Polish National Science Centre (NCN) under Grant Agreement No. DEC-2013/11/B/ST2/04023 and under Postdoctoral Grant No. DEC-2012/04/S/ST2/00003. The work of R. S. is supported by Science and Engineering Research Canada (NSERC).

[1] R. Cahn and S. Dawson, Production of very massive Higgs bosons, Phys. Lett. **136B**, 196 (1984).
[2] D. L. Rainwater and D. Zeppenfeld, Searching for $H \to \gamma\gamma$ in weak boson fusion at the LHC, J. High Energy Phys. 12 (1997) 005.
[3] D. L. Rainwater, D. Zeppenfeld, and K. Hagiwara, Searching for $H \to \tau^+\tau^-$ in weak boson fusion the CERN LHC, Phys. Rev. D **59**, 014037 (1998).
[4] K. Kawade *et al.*, The performance of the LHCf detector for hadronic showers, J. Instrum. **9**, P03016 (2014).
[5] FP420 R and D Collaboration, M. Albrow *et al.*, The FP420 & Project: Higgs and new physics with forward protons at the LHC, J. Instrum. **4**, T10001 (2009).
[6] P. J. Fox, R. Harnik, J. Kopp, and Y. Tsai, Missing energy signatures of dark matter at the LHC, Phys. Rev. D **85**, 056011 (2012).
[7] ATLAS Collaboration, Search for new phenomena in monojet plus missing transverse momentum final states using 10fb-1 of pp collisions at sqrts = 8 TeV with the ATLAS detector at the LHC, https://inspirehep.net/record/1230004?ln=en.
[8] CMS Collaboration, V. Khachatryan *et al.*, Search for dark matter, extra dimensions, and unparticles in monojet events in proton-proton collisions at $\sqrt{s} = 8$ TeV, Eur. Phys. J. C **75**, 235 (2015).
[9] J. Chakrabortty, J. Gluza, R. Sevillano, and R. Szafron, Left-right symmetry at LHC and precise 1-loop low energy data, J. High Energy Phys. 07 (2012) 038.
[10] G. Bambhaniya, J. Chakrabortty, J. Gluza, M. Kordiaczyńska, and R. Szafron, Left-right symmetry and the charged Higgs bosons at the LHC, J. High Energy Phys. 05 (2014) 033.
[11] G. Bambhaniya, J. Chakrabortty, J. Gluza, T. Jeliński, and M. Kordiaczyńska, Lowest limits on the doubly charged Higgs boson masses in the minimal left-right symmetric model, Phys. Rev. D **90**, 095003 (2014).
[12] R. Mohapatra and J. C. Pati, A natural left-right symmetry, Phys. Rev. D **11**, 2558 (1975).
[13] G. Senjanovic and R. N. Mohapatra, Exact left-right symmetry and spontaneous violation of parity, Phys. Rev. D **12**, 1502 (1975).
[14] R. Mohapatra, *Unification and Supersymmetry. The Frontiers of Quark-Lepton Physics* (Springer, New York, 1986).
[15] R. N. Mohapatra and G. Senjanovic, Neutrino masses and mixings in gauge models with spontaneous parity violation, Phys. Rev. D **23**, 165 (1981).
[16] J. Gunion, J. Grifols, A. Mendez, B. Kayser, and F. I. Olness, Higgs bosons in left-right symmetric models, Phys. Rev. D **40**, 1546 (1989).
[17] P. Duka, J. Gluza, and M. Zrałek, Quantization and renormalization of the manifest left-right symmetric model of electroweak interactions, Ann. Phys. (N.Y.) **280**, 336 (2000).
[18] Y. Zhang, H. An, X. Ji, and R. N. Mohapatra, General *CP* violation in minimal left-right symmetric model and constraints on the right-handed scale, Nucl. Phys. **B802**, 247 (2008).
[19] A. Melfo, M. Nemevsek, F. Nesti, G. Senjanovic, and Y. Zhang, Type II seesaw at LHC: The roadmap, Phys. Rev. D **85**, 055018 (2012).
[20] CMS Collaboration, V. Khachatryan *et al.*, Search for heavy neutrinos and W bosons with right-handed couplings in proton-proton collisions at sqrt(s) = 8 TeV, Eur. Phys. J. C **74**, 3149 (2014).
[21] N. D. Christensen and C. Duhr, FeynRules—Feynman rules made easy, Comput. Phys. Commun. **180**, 1614 (2009).
[22] C. Degrande, C. Duhr, B. Fuks, D. Grellscheid, O. Mattelaer, and T. Reiter, UFO—The Universal FeynRules Output, Comput. Phys. Commun. **183**, 1201 (2012).
[23] M. L. Mangano, M. Moretti, F. Piccinini, R. Pittau, and A. D. Polosa, ALPGEN, a generator for hard multiparton processes in hadronic collisions, J. High Energy Phys. 07 (2003) 001.
[24] J. Alwall, M. Herquet, F. Maltoni, O. Mattelaer, and T. Stelzer, MadGraph 5: Going Beyond, J. High Energy Phys. 06 (2011) 128.
[25] T. Sjostrand, S. Mrenna, and P. Z. Skands, PYTHIA 6.4 Physics and Manual, J. High Energy Phys. 05 (2006) 026.
[26] CMS Collaboration, A. Massironi, VBS/VBF from CMS, arXiv:1409.2990.
[27] B. Dutta, R. Eusebi, Y. Gao, T. Ghosh, and T. Kamon, Exploring the Doubly Charged Higgs of the Left-Right

Symmetric Model using Vector Boson Fusion-like Events at the LHC, Phys. Rev. D **90**, 055015 (2014).
[28] C. Englert, E. Re, and M. Spannowsky, Pinning down Higgs triplets at the LHC, Phys. Rev. D **88**, 035024 (2013).
[29] M. Czakon, M. Zrałek, and J. Gluza, Left-right symmetry and heavy particle quantum effects, Nucl. Phys. **B573**, 57 (2000).
[30] M. Czakon, J. Gluza, F. Jegerlehner, and M. Zrałek, Confronting electroweak precision measurements with new physics models, Eur. Phys. J. C **13**, 275 (2000).
[31] M. Czakon, J. Gluza, and J. Hejczyk, Muon decay to one loop order in the left-right symmetric model, Nucl. Phys. **B642**, 157 (2002).
[32] ATLAS Collaboration, G. Aad *et al.*, Search for anomalous production of prompt same-sign lepton pairs and pair-produced doubly charged Higgs bosons with $\sqrt{s} = 8$ TeV pp collisions using the ATLAS detector, J. High Energy Phys. 03 (2015) 041.
[33] G. Ecker, W. Grimus, and H. Neufeld, Higgs induced flavor changing neutral interactions in $\mathrm{SU}(2)_L \times \mathrm{SU}(2)_R \times \mathrm{U}(1)$, Phys. Lett. **127B**, 365 (1983).
[34] R. N. Mohapatra, G. Senjanovic, and M. D. Tran, Strangeness changing processes and the limit on the right-handed gauge boson mass, Phys. Rev. D **28**, 546 (1983).
[35] M. Pospelov, FCNC in left-right symmetric theories and constraints on the right-handed scale, Phys. Rev. D **56**, 259 (1997).
[36] A. Maiezza, M. Nemevsek, F. Nesti, and G. Senjanovic, Left-right symmetry at LHC, Phys. Rev. D **82**, 055022 (2010).
[37] S. Bertolini, A. Maiezza, and F. Nesti, Present and Future K and B Meson Mixing Constraints on TeV Scale Left-Right Symmetry, Phys. Rev. D **89**, 095028 (2014).
[38] D. Guadagnoli and R. N. Mohapatra, TeV scale left right symmetry and flavor changing neutral Higgs effects, Phys. Lett. B **694**, 386 (2011).
[39] J. Chakrabortty, P. Konar, and T. Mondal, Copositive criteria and boundedness of the scalar potential, Phys. Rev. D **89**, 095008 (2014).
[40] A. Datta and A. Raychaudhuri, Mass bounds for triplet scalars of the left-right symmetric model and their future detection prospects, Phys. Rev. D **62**, 055002 (2000).
[41] G. Bambhaniya, J. Chakrabortty, S. Goswami, and P. Konar, Generation of neutrino mass from new physics at TeV scale and multi-lepton signatures at the LHC, Phys. Rev. D **88**, 075006 (2013).
[42] J. Pumplin, D. R. Stump, J. Huston, H.-L. Lai, P. Nadolsky, and W.-K. Tung, New generation of parton distributions with uncertainties from global QCD analysis, J. High Energy Phys. 07 (2002) 012.
[43] W. Barletta, M. Battaglia, M. Klute, M. Mangano, S. Prestemon *et al.*, Working Group Report: Hadron Colliders, arXiv:1310.0290.
[44] R. Assmann, R. Bailey, O. Brüning, O. D. Sanchez, G. de Rijk, J. M. Jimenez, S. Myers, L. Rossi, L. Tavian, E. Todesco, and F. Zimmermann, First thoughts on a higher-energy LHC, Tech. Report No. CERN-ATS-2010-177, CERN, 2010.
[45] Future Circular Collider, http://cern.ch/fcc.
[46] FCC on CERN Document Server, http://cds.cern.ch/collection/Future Circular Collider Documents?ln=en.
[47] F. Z. Johannes Gutleber and Michael Benedikt, Study Brief February 2015, http://cds.cern.ch/record/1994232/.
[48] FCC Week 2015, http://indico.cern.ch/event/340703/.
[49] J. C. Vasquez, Right-handed lepton mixings at the LHC, arXiv:1411.5824.
[50] S. Catani, L. Cieri, G. Ferrera, D. de Florian, and M. Grazzini, Vector Boson Production at Hadron Colliders: A Fully Exclusive QCD Calculation at NNLO, Phys. Rev. Lett. **103**, 082001 (2009).
[51] T. Han, B. Mukhopadhyaya, Z. Si, and K. Wang, Pair production of doubly-charged scalars: Neutrino mass constraints and signals at the LHC, Phys. Rev. D **76**, 075013 (2007).
[52] P. Fileviez Perez, T. Han, G. y. Huang, T. Li, and K. Wang, Neutrino masses and the CERN LHC: Testing type II seesaw, Phys. Rev. D **78**, 015018 (2008).
[53] C. Englert, E. Re, and M. Spannowsky, Triplet Higgs boson collider phenomenology after the LHC, Phys. Rev. D **87**, 095014 (2013).
[54] Z. Kang, J. Li, T. Li, Y. Liu, and G.-Z. Ning, Light doubly charged Higgs boson via the Di-W channel at LHC, arXiv:1404.5207.
[55] S. Kanemura, M. Kikuchi, K. Yagyu, and H. Yokoya, Bounds on the mass of doubly-charged Higgs bosons in the same-sign diboson decay scenario, Phys. Rev. D **90**, 115018 (2014).